Received: March 8, 2024. Revised: March 28, 2024.

International Journal of
Intelligent Engineering & Systems

http://www.inass.org/

Hardware-in-the-Loop Simulation of Grid Connected Modular Multilevel Converter Using Real Time Simulators

Shivashanker K[1] **Janaki M[1]***

[1]*School of Electrical Engineering, Vellore Institute of Technology, Vellore, Tamil Nadu, India.*
* Corresponding author's Email: janaki.m@vit.ac.in

Abstract: The process of designing and controlling modular multilevel converter (MMC) poses numerous challenges. So, hardware-in-the-loop (HIL) simulation and transient analysis are necessary to test the efficacy and reliability of MMC in different operational conditions. This paper presents transient analysis of MMC using MATLAB/Simulink, and results are verified using HIL simulation to validate the performance of decoupled current and circulating current controllers in real-time (RT). The decoupled current control enables the independent control of real and reactive power in AC system, and circulating current control minimizes the circulating currents in MMC phase-legs. The transient analysis is performed on the study system with a rating of 1000 MVA, 220 kV in MATLAB/Simulink. The analysis is carried out for a step perturbation of 100 MW in the real power and 2.0 kA in reactive current references, and results show the satisfactory responses with MMC controllers. The simulation results are validated with HIL simulation of MMC using two RT simulators. The HIL simulation results show the satisfactory responses with closely matching responses to MATLAB/Simulink results.

Keywords: dSPACE, Hardware-in-the-loop (HIL) simulation, Modular multilevel converter (MMC), Transient simulation, Typhoon HIL.

1. Introduction

Modular multilevel converter (MMC) is an advanced power electronic converter architecture for high-voltage (HV) and high-power applications is proposed in [1], like long-distance power transmission, grid-connected renewable energy systems, and electric vehicles. The MMC has superior features like greater operational reliability, significantly lower total harmonic distortion (THD), simple adaptation of voltage levels for each phase, lower switching losses due to lower frequency switching, elimination of filter usage, significant output voltage, redundancy, and modularity [2-5]. These operating advantages make the MMC attractive for use in power systems that regulate power flow and conversion.

According to the literature, the design of resilient MMC controllers requires a systematic approach to provide satisfactory MMC performance under different operating modes. On the other hand, the nonlinear switching components of a MMC make controller design more difficult. Linear modeling using *D-Q* variables is a popular method for designing efficient control strategies for MMCs [6-9]. It is notable that the decoupled control technique on the MMC, using *D-Q* variables, allows for the independent regulation of real and reactive powers. Nonetheless, in order to verify the efficiency of controllers in the presence of nonlinear dynamics, it is essential to include the switching devices with the MMC. However, the design of 3-Φ MMC poses several difficulties such as an immense number of elements, its intricate nature, switching effects, and non-linearities. Hence HIL simulation and transient analysis are necessary to test the efficacy and reliability of MMC in different operational conditions.

From the literature, it is notified that very few articles on transient analysis of MMC connected to grid for HIL simulation. HIL simulation is an approach that combines physical hardware that communicates with the simulated system with real-time system simulation. Additionally, HIL simulation provides a number of advantages, including reduced development time and expense, improved safety and dependability, and enhanced adaptability and scalability [10]. A HIL real-time ultra high-voltage direct current (UHVDC) validation model is set up in [11] by connecting a prototype controller based on dSPACE 1103 to a real-time simulator of OPAL-RT. The real-time simulator runs the power electronics and system components. The prototype controller is used to implement the control component. The design, implementation, and testing of a wind turbine emulation (WTE) system employing a squirrel cage induction motor (SCIM) functioning in DTC mode through HIL are presented in [12] using the dSPACE MicroLab Box and Typhoon HIL 402. A HIL platform for two-terminal MMC systems based on RT-LAB is developed in [13], and the results of steady-state and dynamic performance are desirable. A power-HIL for a medium-voltage, high power, high-speed synchronous motor drive is dis cussed in [14] analytically and experimentally in steady-state and transient-state conditions. In [3], the MATLAB/Simulink modeling of grid connected 3-Φ MMC based back-to-back HVDC system with decoupled current controller is presented. The performance of back-to-back MMC based HVDC system with decoupled current controller is analyzed for different operating conditions by transient analysis using MATLAB/Simulink. The MATLAB/Simulink modeling of 3-Φ single MMC integrated into a mathematical model of rest of power system (ROPS) is presented in [4]. The overall system is implemented in real-time (RT) for HIL simulation. The results of transient analysis of 3-Φ MMC with decoupled current controller in HIL simulation shows an acceptable response.

In [15], the HIL simulation for MMC is developed using RT-LAB. The test scheme is developed to evaluate the physical device's control performance, circulating current suppression, and voltage balance control. The active power step and AC/DC fault test are employed to evaluate the control system of MMC-HVDC in D-Q frame of reference. The proposed method verifies the performance of MMC using HIL simulation. The time responses of MMC follow the applied input disturbance. The MMC and its controller are implemented and evaluated under a real-time environment using a HIL simulation in [16]. The time responses of MMC follow the reference signal with proposed method. The responses attained using HIL simulation closely matches the controller's actual behaviour. In [17], circulating current suppression control (CCSC) and modified nearest level modulation (NLM) approaches are implemented to the MMC using HIL simulation. The proposed methods show satisfactory control over the internal dynamics of the MMC and produce 4N+1 levels. The responses of MMC show the effectiveness of the proposed control methods in HIL simulation.

In references [3, 4], the circulating current controller for MMC is not discussed. In HIL simulation, the circulating current control is not implemented [4]. From references [15-17], it is noticed that the real power and reactive power are controlled in AC system using D-Q components of MMC currents.

This paper presents the modeling of grid connected MMC, and its controllers comprising decoupled current controller and circulating current controller using MATLAB/Simulink. In the design of controller using in-phase and quadrature (P-R) components [18], the control design allows for independent control of real power and reactive power. This is particularly advantageous in applications where precise control of both power components is essential, such as grid-connected converters. In this paper, the real power and reactive power are controlled using P-R components of MMC currents. The objective of our work is to design power decoupled control of the fundamental current and circulating current control. The power decoupled control is achieved through controlling real current and reactive current components which are in phase

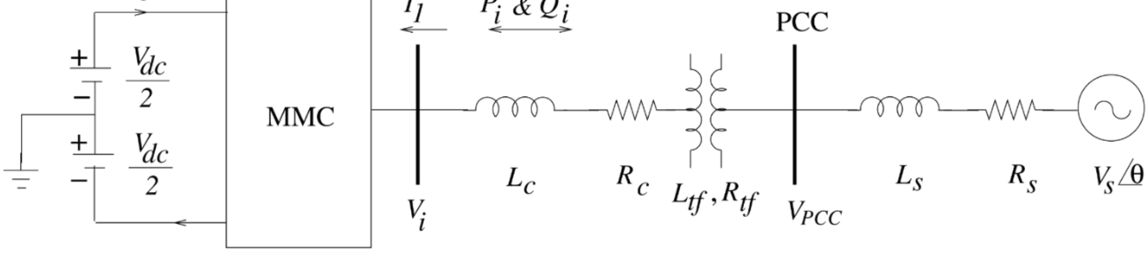

Figure. 1 System diagram of MMC connected to grid

Received: March 8, 2024. Revised: March 28, 2024.

and quadrature with PCC voltage, respectively. The actual value of real current is compared with reference value generated by real power controller. From the time responses, it is evident that the real current and reactive current output of MMC well follow the reference values. The step response of real power output of MMC is faster and closely matching with real power reference. Also, the step response of all signals of MMC is satisfactory. The results of MATLAB/Simulink are verified using HIL simulation to validate the performance of decoupled current controller and circulating current controller in real-time. The PSC-PWM method to produce the pulses to MMC and controllers for MMC strategies are implemented in dSPACE 1202 platform while the MMC 3-Φ model is implemented in Typhoon HIL platform. The decoupled current control enables the independent control of real and reactive power in AC system, while circulating current control minimizes the circulating currents between the arms of each MMC phase-leg. In this paper, transient analysis of MMC connected to the grid using MATLAB/Simulink is performed for two cases, a step perturbation in the real power, and reactive current references. The transient analysis of MMC results show that the satisfactory responses with MMC controllers using MATLAB/Simulink. The simulation results are validated using HIL simulation in two RT simulators. The HIL simulation of the study system is performed with the integration of analog and digital signals (AOs and DIOs) between the dSPACE 1202 MicroLab Box (through control desk) and Typhoon HIL 402 hardware (through HIL SCADA). The transient analysis of HIL simulation for MMC connected to the grid results show satisfactory responses with MMC controllers using two RT simulators to MATLAB/Simulink results.

The rest of the paper is organized as, Section 2 explores the modeling of MMC 3-Φ model, its controller design, Section 3 illustrates the transient analysis of MMC using MATLAB/Simulink, Section 4 presents the HIL simulation of MMC connected to the grid using dSPACE and Typhoon HIL and experimental results, Section 5 provides the conclusions.

2. Modeling of the study system using MATLAB/Simulink

The transient analysis of MMC and HIL simulation for MMC connected to the grid requires detailed MMC 3-Φ model and controllers for MMC in *D-Q* variables. To investigate the transient analysis of MMC on study system is shown Fig. 1. The modeling of MMC 3-Φ model and controllers for MMC using MATLAB/Simulink are presented in the following subsections.

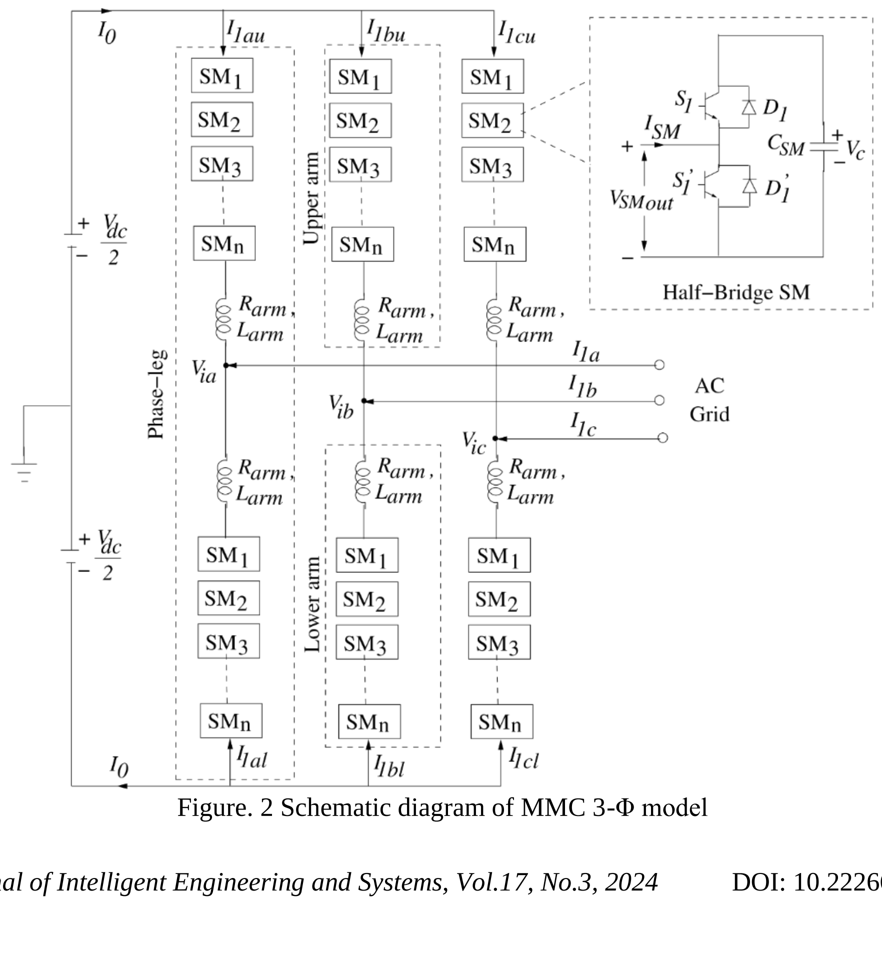

Figure. 2 Schematic diagram of MMC 3-Φ model

Received: March 8, 2024. Revised: March 28, 2024.

2.1 Modeling of 3-Φ MMC

The transient analysis of MMC on study system is analyzed using 3-Φ model of MMC. Fig. 2 shows the schematic representation of MMC 3-Φ model [4]. As depicted in Fig. 2, there are three phase-legs in the MMC. A phase-leg is framed by two arms (lower and upper), each of which consists of '*n*' half-bridge sub-modules (HBSMs) connected in a cascade manner and one series inductor. A series inductor controls the circulating currents with double fundamental frequency components between the upper and lower phase-leg arms. The HBSM is an MMC building block made up of one shunt capacitor and two switches (IGBTs) connected in series. The IGBTs are complementary in functioning to one another based on their gate signals. Table 1 shows the operation of HBSM [4]. The 3-Φ MMC model's switching functions are generated using a phase shifted carrier-based pulse width modulation (PSC-PWM) approach [5].

Table 1. Function of HBSM

Switch, S_1	**Switch, S_1'**	**HBSM output (V_{SMout})**
ON	OFF	V_c
OFF	ON	0

2.2 Designing of MMC controllers

The MMC controllers are designed to control the real and reactive power independently in AC system, and to suppress circulating currents flowing between lower and upper arms of each MMC phase-legs. The subsequent subsections elaborate on the architecture of MMC controllers.

2.2.1. Decoupled current control

The decoupled current control scheme [9] is used to control the real and reactive powers independently.

The architecture of decoupled current control is shown in Fig. 3. Referring to Fig. 3, the reference value of real current, I_{1PRef} is attained from the real power controller. The reference value of reactive

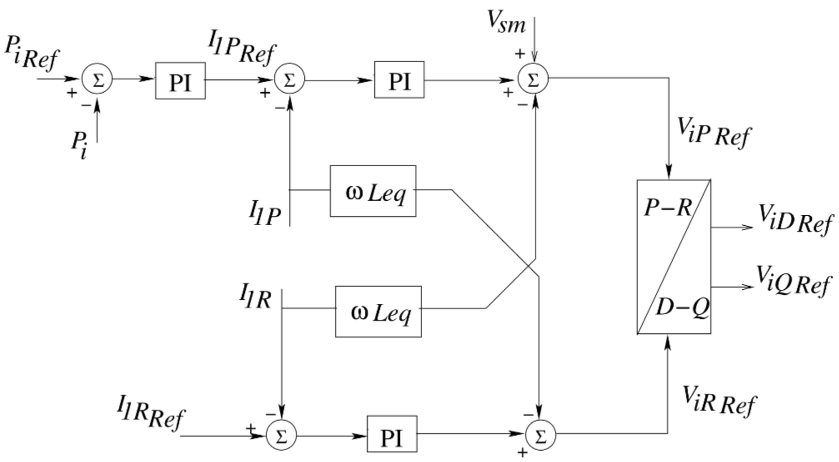

Figure. 3 Decoupled current controller for 3-Φ MMC

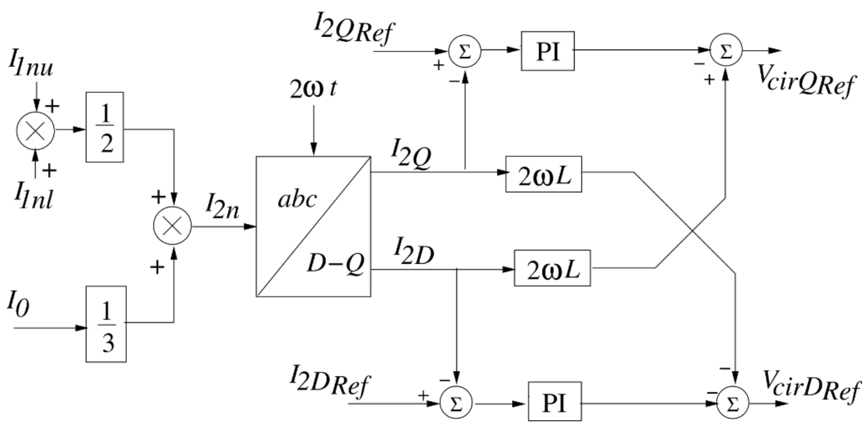

Figure. 4 Circulating current controller for 3-Φ MMC

Received: March 8, 2024. Revised: March 28, 2024.

current, I_{1RRef} is kept constant or attained from AC bus voltage controller. The measured real, I_{1P} and reactive, I_{1R} currents are calculated from MMC *D-Q* current (I_{1D} and I_{1Q}) components. The decoupled controller controls the P_i and Q_i effectively and independently. Therefore, enhance the MMC's dynamic response. However, the controller's parameters affect the MMC response, and they are adjusted based on the intended output for the perturbation given to the input. The computed values of P_i and Q_i supplied by MMC are shown below.

$$P_i = V_{iD}I_{1D} + V_{iQ}I_{1Q} \tag{1}$$

$$Q_i = V_{iD}I_{1Q} - V_{iQ}I_{1D} \tag{2}$$

From the Fig. 3, the output voltage of the MMC is represented in the *D-Q* frame of reference [9] as follows:

$$V_i = \sqrt{V_{iD}^2 + V_{iQ}^2} \tag{3}$$

$$V_{iD} = V_{iR}cos\theta + V_{iP}sin\theta \tag{4}$$

$$V_{iQ} = -V_{iR}sin\theta + V_{iP}cos\theta \tag{5}$$

The MMCs real and reactive current components are given by the following equations

$$I_{1P} = I_{1D}sin\theta + I_{1Q}cos\theta \tag{6}$$

$$I_{1P} = I_{1D}sin\theta + I_{1Q}cos\theta \tag{7}$$

2.2.2. Circulating current control

The circulating current controller is used to minimize the circulating currents flows in the arms of each phase-leg of MMC.

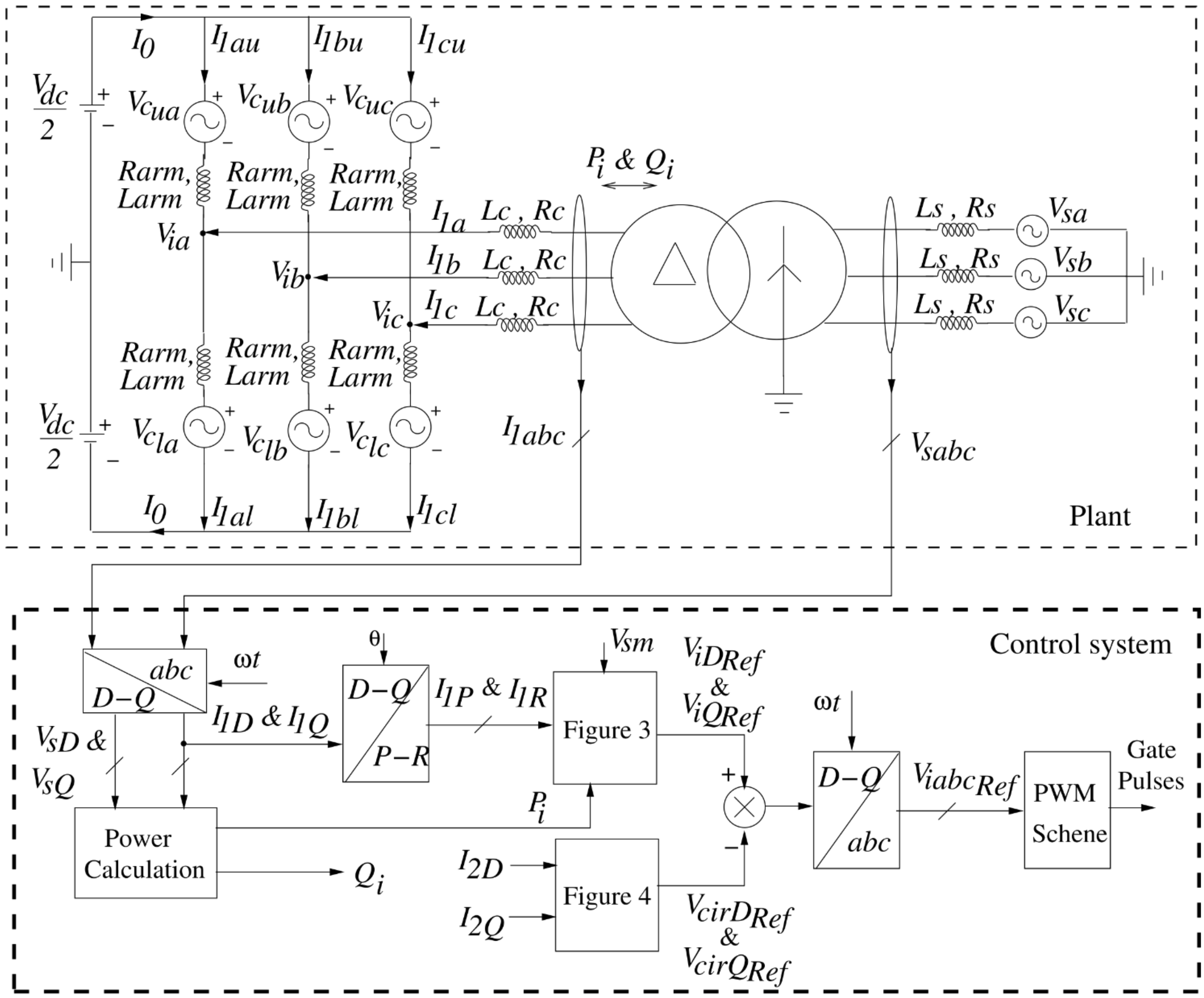

Figure. 5 Architecture of study system with control system

 DOI: 10.22266/ijies2024.0630.40

Fig. 4 shows the architecture of circulating current controller for MMC [19]. The circulating currents are produced in each phase-leg of 3-Φ MMC due to the inner voltage difference between the lower and upper arms.The circulating currents have a negative sequence with a frequency of two times the fundamental frequency, and doesn't affect the AC-side currents and voltages [20]. The presence of second harmonic currents leads to arise in the rms values of the arm currents, resulting in greater power losses in the MMC [21]. These currents comprising of one third of the total DC current ($\frac{I_0}{3}$) and AC current corresponding to double fundamental frequency. The circulating currents flowing through each phase-leg in 3-Φ variables are given below as,

$$I_{2n} = \frac{I_0}{3} + \frac{(I_{1nu} + I_{1nl})}{2} \quad (8)$$

where, *n*=phase - *a*, *b*, and *c*

The three-phase circulating currents are trans formed into D-Q variables (I_{2D} and I_{2Q}) using negative-sequence rotational reference frame with double fundamental frequency [5] as shown in Fig. 4.

3. Transient analysis of MMC on the study system using MATLAB/Simulink

The effect of controllers for MMC and 3-Φ MMC performance on the study system are analyzed with MATLAB/Simulink. The architecture of study system with control system is shown in Fig. 5. To design the controllers for MMC in *D-Q* variables, the 3-Φ grid voltages and MMC currents are transformed into *D-Q* variables with Kron's transformation [9]. The transient analysis of 3-Φ MMC is per formed for two cases, a step perturbation in the real power, and reactive current references are explained in subsequent sections.

3.1 Step perturbation in real power reference (P_{iRef})

In this section the transient analysis of MMC on the study system is explored when the step perturba-tion in the real power reference, P_{iRef} is employed. The transient response of real power, P_i, real current, I_{1P}, reactive current, I_{1R}, reactive power, Q_i, and circulating current com ponents, I_{2D} and I_{2Q} for case-1 with MMC 3-Φ model are shown in Figs. 6-10. From the Fig. 6, it is clear that P_i change from rectifier mode (100 MW) to inverter mode (-100 MW) at employing step perturbation in P_{iRef} and changing from inverter mode (-100 MW) to rectifier mode (100 MW) at restoring the perturbation in P_{iRef}. The response shows that fast transition from rectifier to inverter and vice-versa, and the transient response of the P_i is satisfactory. Referring to Fig. 7, it is clear that the time response of I_{1P} is changed from 0.2 kA to -0.2 kA at employing step perturbation in P_{iRef} and changing from -0.2 kA to 0.2 kA at restoring the perturbation in P_{iRef}. Therefore, the time responses show the I_{1P} has followed the step perturbation in P_{iRef}. From the Figs. 8 and 9, it is clear that the time responses of I_{1R} and Q_i are not affected from step perturbation in P_{iRef}. Referring to Figs. 10 and 11, it is clear that the time responses of I_{2D} and I_{2Q} are not affected from step perturbation in P_{iRef} and observed that the circulating currents are minimized in MMC phase-legs.

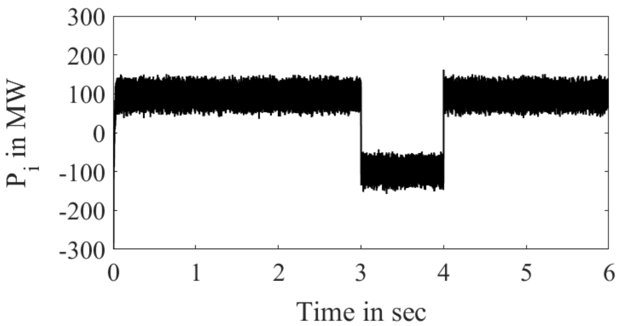

Figure. 6 Case-1: Response of real power (P_i) with MMC 3-Φ model for step perturbation in P_{iRef}

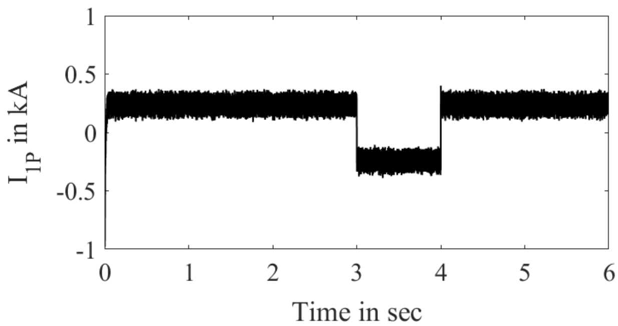

Figure. 7 Case-1: Response of real current (I_{1P}) with MMC 3-Φ model for step perturbation in P_{iRef}

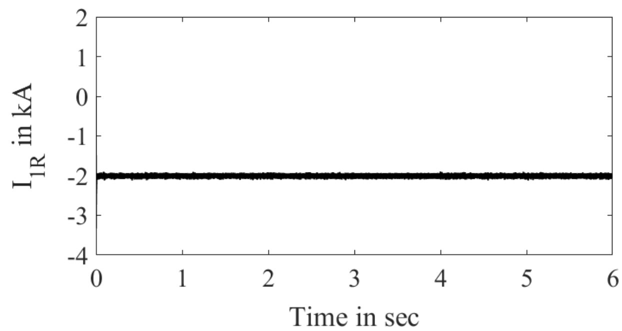

Figure. 8 Case-1: Response of reactive current (I_{1R}) with MMC 3-Φ model for step perturbation in P_{iRef}

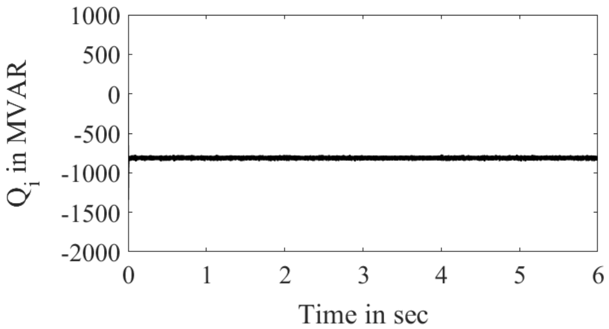

Figure. 9 Case-1: Response of reactive power (Q_i) with MMC 3-Φ model for step perturbation in P_{iRef}

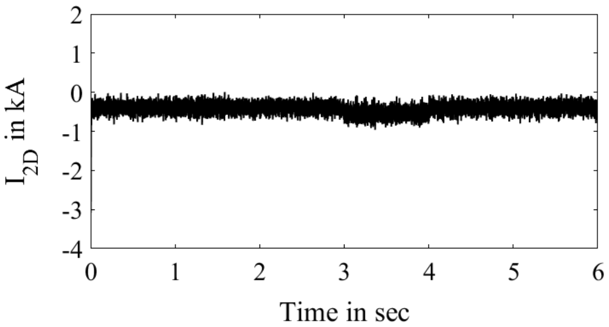

Figure. 10 Case-1: Response of circulating current component (I_{2D}) with MMC 3-Φ model for step perturbation in P_{iRef}

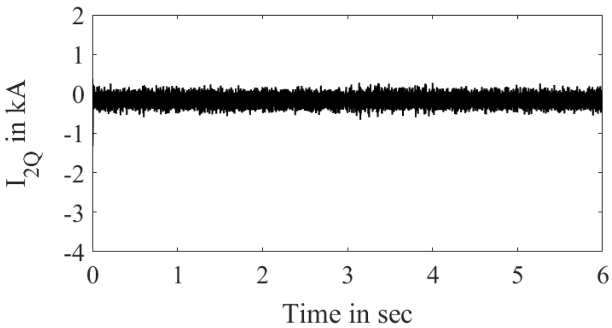

Figure. 11 Case-1: Response of circulating current component (I_{2Q}) with MMC 3-Φ model for step perturbation in P_{iRef}

3.2 Step perturbation in reactive current reference (I_{1RRef})

In this section the transient analysis of MMC on the study system is explored when the step perturbation in the reactive current reference, I_{1RRef} is employed. The transient response of real power, P_i, real current, I_{1P}, reactive current, I_{1R}, reactive power, Q_i, and circulating current components, I_{2D} and I_{2Q} for case-2 with MMC 3-Φ model are shown in Figs. 12-17. From the Figs. 12 and 13, it is clear that the responses of P_i and I_{1P} are not affected from step perturbation in I_{1RRef}. Referring to Fig. 14, it is clear that I_{1R} changed from capacitive mode (-2.00 kA) to inductive mode (2.00 kA) at step perturbation in I_{1RRef}

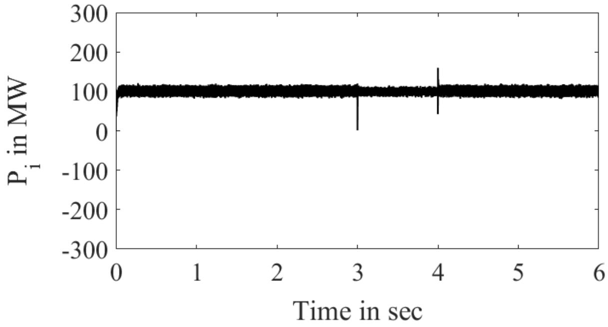

Figure. 12 Case-2: Response of real power (Pi) with MMC 3-Φ model for step perturbation in I_{1RRef}

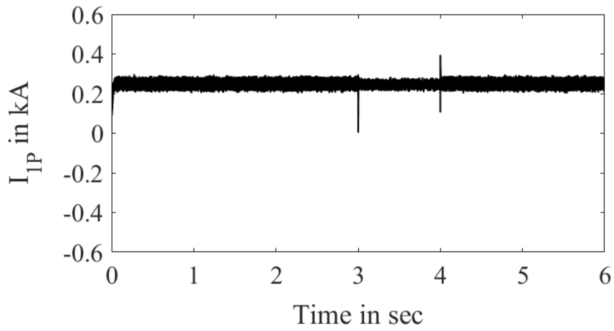

Figure. 13 Case-2: Response of real current (I1P) with MMC 3-Φ model for step perturbation in I_{1RRef}

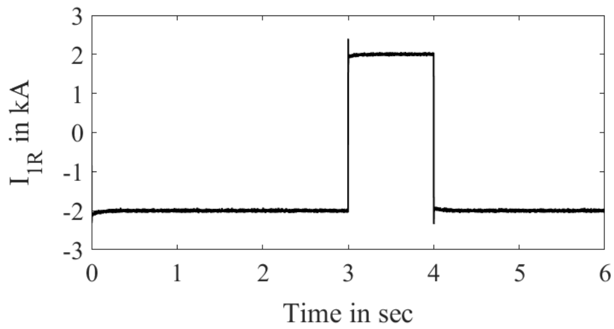

Figure. 14 Case-2: Response of reactive current (I_{1R}) with MMC 3-Φ model for step perturbation in I_{1RRef}

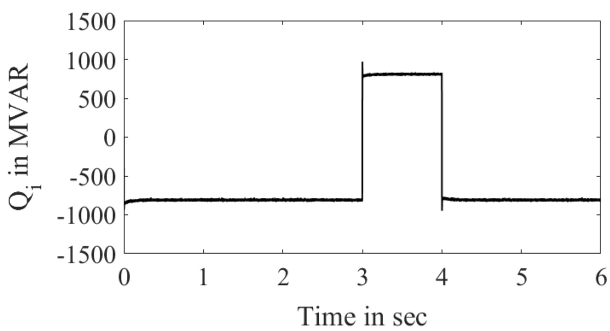

Figure. 15 Case-2: Response of reactive power (Q_i) with MMC 3-Φ model for step perturbation in I_{1RRef}

Received: March 8, 2024. Revised: March 28, 2024.

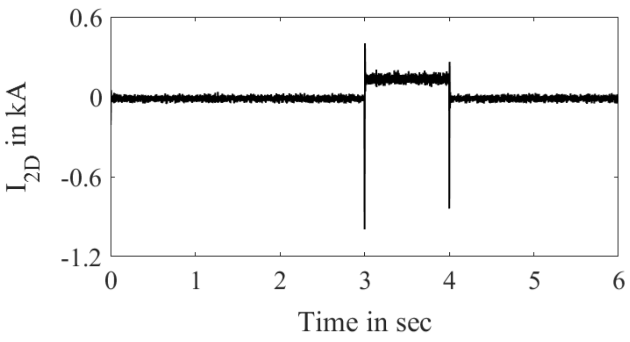

Figure. 16 Case-2: Response of circulating current component (I_{2D}) with MMC 3-Φ model for step perturbation in I_{1RRef}

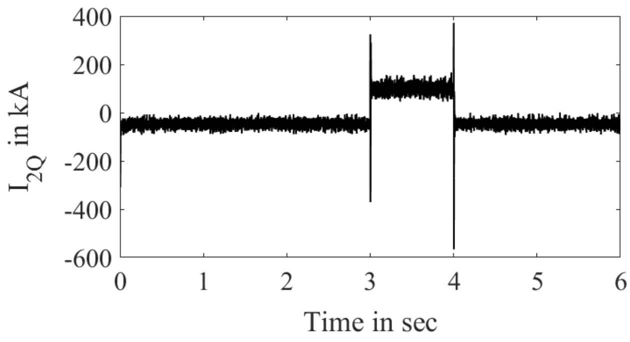

Figure. 17 Case-2: Response of circulating current component (I_{2Q}) with MMC 3-Φ model for step perturbation in I_{1RRef}.

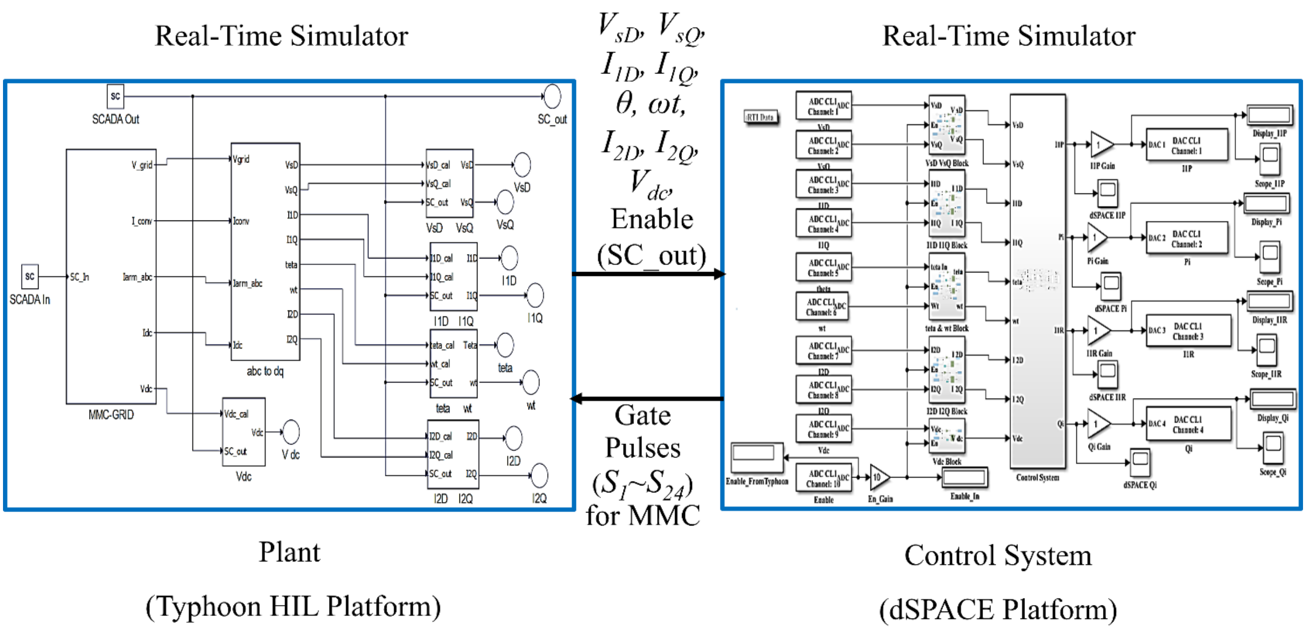

Figure. 18 HIL simulation block diagram of MMC connected to grid

and changing from inductive mode (2.00 kA) to capacitive mode (-2.00 kA) at restoring the perturbation in I_{1RRef}. The response shows that fast transition from capacitive to inductive and vice-versa and the response of the I_{1R} is satisfactory. From the Fig. 15, it is noticed that the response of Q_i is changed from -800 MVAR to 800 MVAR at employing step perturbation in I_{1RRef} and changing from 800 MVAR to -800 MVAR at restoring the perturbation in I_{1RRef}. Therefore, the response show the Q_i has followed the step perturbation in I_{1RRef}. Referring to Figs. 16 and 17, it is clear that the time responses of I_{2D} and I_{2Q} are affected from step perturbation in I_{1RRef} and observed that the circulating currents are not minimized in MMC phase-legs during step perturbation employed and restored time.

4 Modeling of study system for HIL simulation using dSPACE and Typhoon HIL and Result Analysis

The study system of HIL simulation for transient analysis of the MMC connected to grid as shown in Fig. 5 is developed in two well-known RT simulators such as Typhoon HIL and dSPACE platform as shown in Fig. 18. The subsequent subsections explain the modeling of the study system using two RT platforms for HIL simulation.

4.1 Modeling of MMC 3-Φ model in Typhoon HIL platform

The transient analysis is performed using 3-Φ model of MMC connected to grid developed in Typhoon HIL 402 platform. The Typhoon HIL is a platform that employs field programmable gate array (FPGA) technology to simulate power system and power electronic systems in real-time with high fidelity. The following steps explains the modeling of 3-Φ MMC in Typhoon HIL.

- Modeling of the 3-Φ MMC connected to grid using library blocks in Typhoon HIL Schematic Editor as shown in Fig. 18, and which is used to build high-fidelity models of the power stage for real-time simulations.
- Compile the model using Typhoon HIL tools, such as Compiler or Simulator. Then model is executed in RT on a Typhoon HIL402 hardware and opens the HIL SCADA panel.
- HIL SCADA panel provides a interface between Schematic Editor and Typhoon HIL 402 hard ware.
- HIL SCADA panel enables the control of input and output signals from and to external devices using HIL SCADA widgets like analog input output (AIO) and digital input-output (DIO) settings.
- The required AIO and DIO signals connected from Typhoon HIL 402 hardware to dSPACE 1202 MicroLab Box to make HIL simulation.

4.2 Designing of MMC controllers in dSPACE platform

The controllers for MMC are developed to control the real and reactive power independently in AC system, and to suppress circulating currents flowing between lower and upper arms of each MMC phase-legs. This section presents the designing of controllers for MMC and PSC-PWM method using dSPACE 1202 platform as shown in Fig. 18. The dSPACE 1202 is a RT platform which provides a rapid prototyping and implementation of control algorithms for power electronic systems using FPGA technology. The following steps explains the designing of controllers for 3-Φ MMC in dSPACE.

- Designing of control system, comprising decoupled current control, circulating current control, and PSC-PWM method using dSPACE 1202 platform with MATLAB/Simulink library blocks and RT interface blocks.
- Build the control system model and generate code for control system.
- The evaluation of control system, developed in dSPACE 1202 platform is observed/controlled using control desk as interface unit/ panel between dSPACE 1202 platform and MicroLab Box.
- A control desk is an interface panel to access the dSPACE 1202 platform and analyze the control system in RT/online mode.
- A control desk enables the control of input and output signals from and to external devices using MicroLab Box with AIO and DIO ports.
- The required AIO and DIO signals connected from MicroLab Box to Typhoon HIL 402 hard ware to make HIL simulation.

4.3 Transient analysis of MMC on the study system using HIL simulation

The 3-Φ MMC connected to the grid (plant) and its control system comprising decoupled and circulating current controller and PSC-PWM scheme

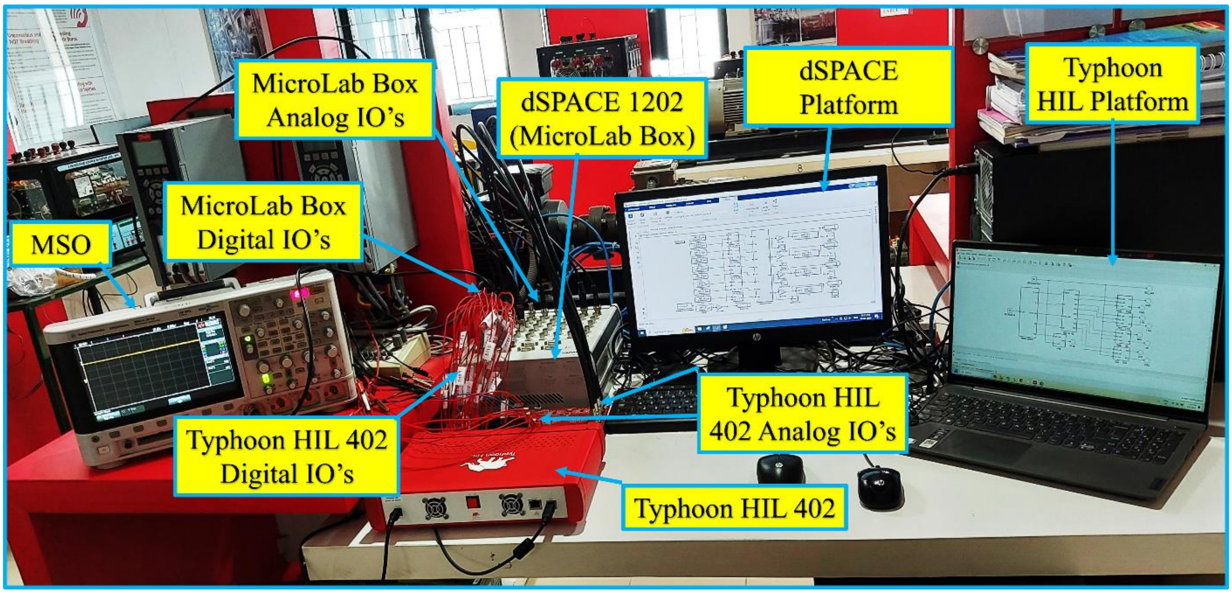

Figure. 19 HIL simulation test setup of MMC connected to grid

Received: March 8, 2024. Revised: March 28, 2024.

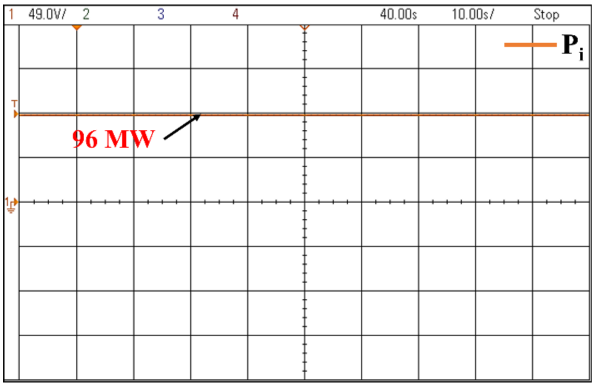

Figure. 20 Real-time simulation of real power (P_i) with MMC 3-Φ model

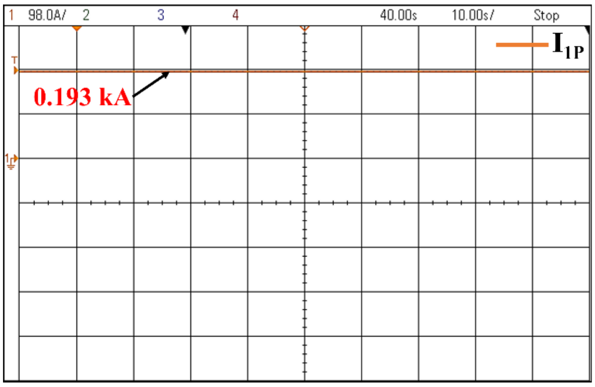

Figure. 21 Real-time simulation of real current (I_{1P}) with MMC 3-Φ model

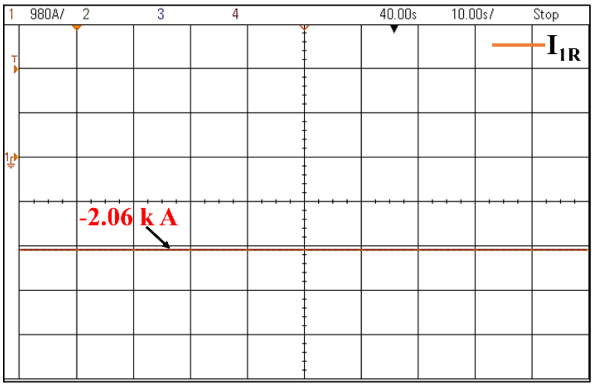

Figure. 22 Real-time simulation of reactive current (I_{1R}) with MMC 3-Φ model

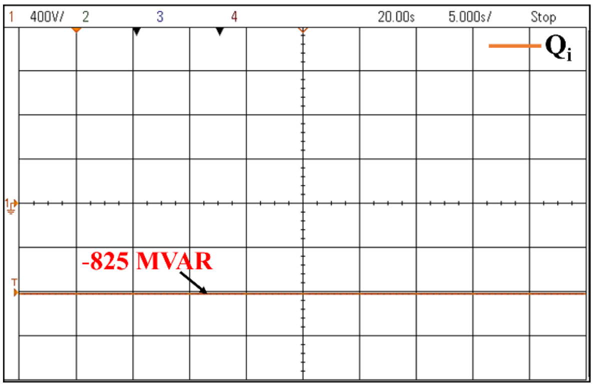

Figure. 23 Real-time simulation of reactive power (Q_i) with MMC 3-Φ model

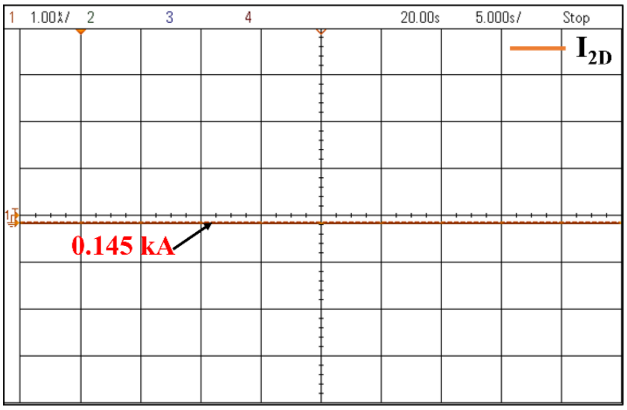

Figure. 24 Real-time simulation of circulating current component (I_{2D}) with MMC 3-Φ model

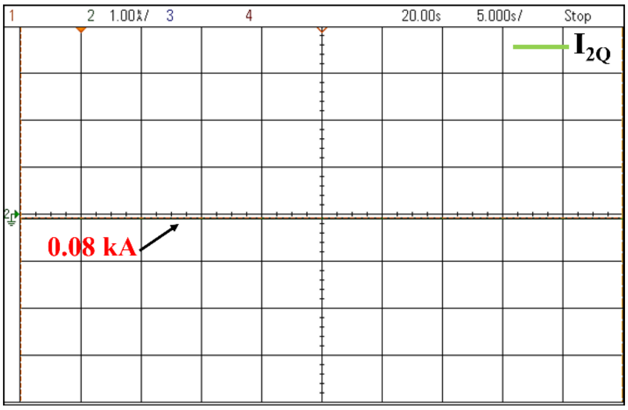

Figure. 25 Real-time simulation of circulating current component (I_{2Q}) with MMC 3-Φ model

are shown in Fig. 5 implemented in two RT simulators, dSPACE 1202 and Typhoon HIL. The HIL simulation for transient analysis of MMC connected to the grid test set up is shown in Fig. 19. The plant and control systems operate independently when the enable signal is low (SC_out=0) between two RT platforms (see Fig. 18). If the enable signal is set to high (SC_out=1) manually, then two RT platforms are interconnected to operate the HIL simulation and perform the transient simulation of the MMC on study system. The HIL simulation for transient analysis of MMC connected to grid response of real power, P_i, real current, I_{1P}, reactive current, I_{1R}, reactive power, Q_i, and circulating current components, I_{2D} and I_{2Q} with MMC 3-Φ model are shown in Figs. 20-25. From the Figs. 20-25, it is clear that the RT response of real power (96 MW, measured in terms of ‘V′, 96 V shown in mixed signal oscilloscope (MSO)), real current (0.193 kA), reactive current (-2.06 kA), reactive power (-825 MVAR, measured in terms of ‘V′, -825 V shown in MSO), circulating current components, I_{2D} (0.145 kA), and I_{2Q} (0.08 kA) are satisfactory with transient simulation of MMC using MATLAB/Simulink results.

5. Conclusion

This paper presents the modeling of 3-Φ MMC and controllers for MMC comprising decoupled and circulating current control. In the design of controller using in-phase and quadrature (P-R) components, the control design allows for independent control of real power and reactive power. This is particularly advantageous in applications where precise control of both power components is essential, such as grid-connected converters. In this paper, the real power and reactive power are controlled using P-R components of MMC currents. The transient analysis of MMC is performed using MATLAB/Simulink and HIL simulation. The transient analysis of MMC connected to the grid using MATLAB/Simulink is performed for two cases, a step perturbation in the real power, and reactive current reference. The simulation results are validated using HIL simulation with two real-time platforms. The dSPACE 1202 is used to implement the controllers for MMC and PSC-PWM technique, Typhoon HIL 402 platform is used to implement 3-Φ MMC connected to the grid (plant) for HIL simulation. The following findings are made with the results of MATLAB/Simulink and HIL simulation of MMC connected to the grid.

- The decoupled current control enables the independent control of real and reactive power in AC system.
- Circulating current components (I_{2D} and I_{2Q}) are minimized for step perturbation in real power reference of MMC.
- The MATLAB/Simulink results of three phase MMC show good step response of real power, real current, reactive current, and reactive power with proposed controllers.
- The HIL simulation results show the satisfactory using two real-time simulators, and closely matches to MATLAB/Simulink results.

Conflicts of Interest

The authors declare no conflict of interest.

Author Contributions

Conceptualization, Shivashanker K and Janaki M; methodology, Shivashanker K; software, Shivashanker K; validation, Janaki M; formal analysis, Shivashanker K; investigation, Janaki M; resources, Janaki M; data curation, Shivashanker K; writing—original draft preparation, Shivashanker K; writing—review and editing, Janaki M; visualization, Shivashanker K; supervision, Janaki M; project administration, Janaki M.

Nomenclature

V_{dc}	DC side voltage
I_0	DC side current
I_{1n}	Fundamental frequency current component of MMC; *n*=phase-*a, b* and *c*
R_{arm}, L_{arm}	Arm resistance and inductance of MMC
L_c, R_c	Line inductance and resistance between MMC and point of common coupling (PCC)
V_{PCC}	PCC voltage
L_{tf}, R_{tf}	Inductance and resistance of transformer
L_s, R_s	Inductance and resistance of source
D, Q	Subscripts to denote direct and quadrature components in network reference frame
θ	Phase angle of source voltage
ω	Ramp of the source voltage
V_{in}	MMC output voltage; *n*=phase-*a, b* and *c*
I_{1nl}, I_{1nu}	Lower and upper arm currents of MMC; *n*=phase-*a, b* and *c*
V_{cln}, V_{cun}	Lower and upper arm voltages of MMC; *n*=phase-*a, b* and *c*
C_{SM}	Submodule (SM) capacitance
I_{SM}	SM current
V_c	SM capacitor voltage
V_{SMout}	SM output voltage
I_{1P}, I_{1R}	Real and reactive components of MMC fundamental frequency current
V_{iP}, V_{iR}	Real and reactive components of MMC voltage
I_{2D}, I_{2Q}	Circulating currents with double fundamental frequency component of MMC
V_{cirD}, V_{cirQ}	MMC circulating voltages
V_{1D}, V_{1Q}	Fundamental frequency component of controlled output voltages of MMC
P_i, Q_i	Real power and reactive power contributed by fundamental frequency component of MMC

References

[1] A. Lesnicar and R. Marquardt, "An innovative modular multilevel converter topology suitable for a wide power range", *IEEE Bologna Power Tech Conference Proceedings*, Bologna, Italy, Vol. 3, 2003.

[2] M. A. Perez, S. Bernet, J. Rodriguez, S. Kouro and R. Lizana, "Circuit Topologies, Modeling,

Control Schemes, and Applications of Modular Multilevel Converters", *IEEE Transactions on Power Electronics*, Vol. 30, No. 1, pp. 4-17, 2015.

[3] K. Shivashanker, M. Janaki and R. Thirumalaivasan, "Design of Decoupled Current Controller for Back to Back Modular Multilevel Converter Based HVDC Transmission System", In: *Proc. of Innovations in Power and Advanced Computing Technologies (i-PACT)*, Kuala Lumpur, Malaysia, pp. 1-5, 2021.

[4] Shivashanker, K and Janaki, M. "An approach on nonlinear integration of mmc to linear model of ROPS in transient analysis", *International Journal of Circuit Theory and Applications*, Vol. 51, No. 10, pp. 4584–4606, 2023.

[5] J. Wang and P. Wang, "Power Decoupling Control for Modular Multilevel Converter", *IEEE Transactions on Power Electronics*, Vol. 33, No. 11, pp. 9296-9309, 2018.

[6] R. Lizana, M. A. Perez, D. Arancibia, J. R. Espinoza and J. Rodriguez, "Decoupled Current Model and Control of Modular Multilevel Converters", *IEEE Transactions on Industrial Electronics*, Vol. 62, No. 9, pp. 5382-5392, 2015.

[7] M. A. Pérez, R. Lizana F. and J. Rodríguez, "Decoupled current control of modular multilevel converter for HVDC applications", In: *Proc. of IEEE International Symposium on Industrial Electronics*, Hangzhou, China, pp. 1979-1984, 2012.

[8] B. Li, Z. Xu, J. Ding and D. Xu, "Decoupled modeling and control of the modular multilevel converter", In: *Proc. of IEEE Applied Power Electronics Conference and Exposition (APEC)*, San Antonio, TX, USA, pp. 3275-3280, 2018.

[9] Shivashanker, K. and M. Janaki, "Design of Decoupled Current Controller for Grid Connected Modular Multilevel Converter", *International Journal of Emerging Trends in Engineering Research*, Vol. 8, No. 8, pp. 4508-4514, 2020.

[10] N. Lin and V. Dinavahi, "Detailed Device-Level Electrothermal Modeling of the Proactive Hybrid HVDC Breaker for Real-Time Hardware-in-the-Loop Simulation of DC Grids," *IEEE Transactions on Power Electronics*, Vol. 33, No. 2, pp. 1118-1134, 2018.

[11] X. Fu, A. Javadi, K. Al-Haddad, L. -A. Dessaint, W. Li and B. -T. Ooi, "HIL-RT Implementation of UHVDC Transmission System Based on Series-Connected VSC Modules", *IEEE Access*, vol. 7, pp. 84602-84612, 2019.

[12] Osama M. Arafa, Mohamed E. Abdallah and Ghada A. Abdel Aziz, "Realisation and HIL testing of wind turbine emulator based on DTC squirrel cage induction motor drive", *International Journal of Industrial Electronics and Drives*, Vol. 4, No. 3, pp. 155-168, 2018.

[13] G. Li, D. Zhang, Y. Xin, S. Jiang, W. Wang and J. Du, "Design of MMC hardware-in-the-loop platform and controller test scheme", *CPSS Transactions on Power Electronics and Applications*, Vol. 4, No. 2, pp. 143-151, 2019.

[14] K. Saito and H. Akagi, "A Power Hardware-in-the-Loop (P-HIL) Test Bench Using Two Modular Multilevel DSCC Converters for a Synchronous Motor Drive", *IEEE Transactions on Industry Applications*, Vol. 54, No. 5, pp. 4563-4573, 2018.

[15] G. Li, D. Zhang, Y. Xin, S. Jiang, W. Wang and J. Du, "Design of MMC hardware-in-the-loop platform and controller test scheme", *CPSS Transactions on Power Electronics and Applications*, Vol. 4, No. 2, pp. 143-151, 2019.

[16] J. A. Ansari, C. Liu and L. Zheng, "Efficient Real-Time Testing of 51 Level MMC Converter in Hardware in Loop (HIL) Setup for HVDC Applications," In: *Proc. of 9th International Conference on Electrical and Electronics Engineering (ICEEE)*, Alanya, Turkey, pp. 27-31, 2022.

[17] J B Soomro, K H Ali and A A Memon, "Hardware-in-the-loop setup for enhanced modular multi-level converter with reduced circulating currents", *International Journal of Electrical and Computer Engineering (IJECE)*, Vol. 14, No. 2, pp. 1448-1458, 2024.

[18] K. R. Padiyar, *FACTS Controllers in Power Transmission and Distribution*, New age International (P) Ltd, 2007.

[19] A. Jamshidifar and D. Jovcic, "Small-Signal Dynamic DQ Model of Modular Multilevel Converter for System Studies", *IEEE Transactions on Power Delivery*, Vol. 31, No. 1, pp. 191-199, 2016.

[20] Q. Tu, Z. Xu, H. Huang and Jing Zhang, "Parameter design principle of the arm inductor in modular multilevel converter based HVDC," In: *Proc. of International Conference on Power System Technology*, Hangzhou, pp. 1-6, 2010.

[21] A. Antonopoulos, L. Angquist and H. -P. Nee, "On dynamics and voltage control of the Modular Multilevel Converter", In: *Proc. of 13th European Conference on Power Electronics and Applications, Barcelona*, Spain, pp. 1-10, 2009.